Colloids and Surfaces, 56 (1991) 119–148
Elsevier Science Publishers B.V., Amsterdam

The van der Waals component of the interfacial bending moment
2. Model development and numerical results

Theodor D. Gurkov, Peter A. Kralchevsky and Ivan B. Ivanov

Laboratory of Thermodynamics and Physico-Chemical Hydrodynamics, University of Sofia, Faculty of Chemistry, Anton Ivanov Avenue 1, 1126 Sofia (Bulgaria)

(Received 13 April 1990; accepted 6 September 1990)

Abstract

A model for calculation of the pressure tensor components is developed on the basis of some general results in the thermodynamics and statistical mechanics of spherical interfaces. The van der Waals intermolecular forces are taken into consideration. The model contains three parameters which are to be found from experiments. These are the interfacial tension of a flat interface and the Hamaker constants of the two neighboring phases. Then the model allows calculation of the interfacial bending moment, of the Tolman length and of the curvature dependence of the interfacial tension. Numerical results are obtained for various liquid-gas and water-oil interfaces at different radii of curvature. The results agree well with statistical-mechanical calculations and computer simulations by other authors. The calculated mechanical and thermodynamical interfacial tensions turn out to differ appreciably for drop radii below 1000 Å owing to the bending moment effect. The results can be applied for calculation of the size distribution and other properties of different fluid dispersions, including microemulsions.

1. INTRODUCTION

The dependence of the liquid–fluid interfacial tension on curvature is important for microheterogeneous systems like microemulsions and critical emulsions – systems of low interfacial tension and high dispersity [1–5]. An obvious problem with these systems is that the interfacial tension of the microscopic droplets is not liable to direct measurement. However, the interfacial tension can affect the equilibrium droplet size distribution [1–3,6,7] and the second virial coefficient [8]. Hence, the droplet interfacial tension and its curvature dependence can in principle be determined indirectly by interpreting experimental data by means of appropriate theoretical models.

In the present paper we consider the interface between two pure immiscible fluids, whose molecules do not exhibit surface activity (like water–air, water–hydrocarbon etc. interfaces). Our purpose is to calculate the contribution of

0166-6622/91/$03.50

the van der Waals forces to the curvature dependence of the interfacial tension σ and to the interfacial bending moment B. This will be done by only using information about the values of the London constants, α_{ij}, of van der Waals interactions and about the limiting value, σ_0, of the interfacial tension at a flat interface. We suppose that σ_0 is known from the experiment, i.e. we will not calculate this value from first principles as done in Refs [9–13]. In fact only the curvature dependence of σ is the subject of our study. We attempt to achieve this purpose by combining some general equations of thermodynamics and statistical mechanics and by developing an appropriate model. All parameters of the model are intended to be determined from the values of α_{ij} and σ_0.

As pointed out in Refs [14,15], one has to distinguish between the mechanical and the thermodynamical interfacial tensions, σ and γ, when dealing with interfaces of high curvature. The relation connecting these two quantities for spherical interface reads [15]

$$\gamma=\sigma+\tfrac{1}{2}BH \tag{1.1}$$

where B is the interfacial bending moment and H is the curvature of the spherical dividing surface of radius a, $H=-1/a$. According to the curvature sign convention (see Eqns (2.18) and (2.19) in Ref. [16] we consider a to be positive for liquid drops in gas and for water drops in oil. On the contrary, a is considered here to be negative (although accounted from the center of curvature) for gas bubbles in liquid and for oil drops in water. Then B is positive when it tends to bend the interface around the liquid phase in the case of liquid–gas systems and around the aqueous phase for oil–water systems – (see Ref. [16]). Therefore, the sign of B is certain to be independent of the sign of curvature.

Equation (1.1) holds for every choice of the dividing surface. Here and hereafter we will assume that a is the radius of the equimolecular dividing surface, and γ, σ and B are the values of the respective quantities for this specified dividing surface.

We consider a spherical drop or bubble, phase I, composed of pure component 1, surrounded by phase II, composed of component 2. The choice of a as radius of the equimolecular dividing surface corresponds to zero adsorption of component 1 (see Section 2 of Part 1, Ref. [14], for more details).

Equation (1.1) shows that the values of γ and σ for a flat interface $(1/a\to 0)$ coincide:

$$\gamma_0=\sigma_0 \tag{1.2}$$

The dependence of γ on a can be expressed by means of the known thermodynamic Gibbs–Tolman formula [17–20]

$$\gamma=\gamma_0\left[1-\frac{2\delta_0}{a}+o\left(\frac{1}{a}\right)\right] \tag{1.3}$$

where δ_0 is the Gibbs–Tolman parameter representing the distance between the equimolecular dividing surface and the surface of tension for a flat interface. One purpose of our model is to calculate δ_0 for different interfaces.

The Gibbs–Tolman parameter is related to the interfacial bending moment of a flat interface, B_0 [16,21]:

$$B_0 = 2\,\gamma_0 \delta_0 \tag{1.4}$$

In view of Eqn (1.4), Eqn (1.3) can be transformed to read

$$\gamma = \gamma_0 - \frac{B_0}{a} + o\left(\frac{1}{a}\right) \tag{1.5}$$

Here the Landau symbol "$o(1/a)$" means that the higher-order terms tend to zero more rapidly than $1/a$ at large a (see for example Ref. [22]). Besides, Eqns (1.1)–(1.5) yield

$$\sigma = \sigma_0\left[1 - \frac{\delta_0}{a} + o\left(\frac{1}{a}\right)\right] = \sigma_0 - \frac{B_0}{2a} + o\left(\frac{1}{a}\right) \tag{1.6}$$

For a spherical interface one has [14,15]

$$\gamma(a) = \tfrac{2}{3}\,\sigma(a) + \tfrac{1}{3}\,J(a) \tag{1.7}$$

where

$$\sigma(a) = \int_0^\infty \Delta P(r,a)\,\frac{a}{r}\,\mathrm{d}r \tag{1.8}$$

is the mechanical interfacial tension and

$$J(a) = \int_0^\infty \Delta P(r,a)\,\frac{r^2}{a^2}\,\mathrm{d}r \tag{1.9}$$

is an auxiliary notation. It is seen that an expression for $\Delta P(r,a)$ is needed in order to find $\sigma(a)$ and $\gamma(a)$. In acccordance with Part 1 [14] we seek a model expression for $\Delta P(r,a)$, satisfying the following general physical conditions: (i) to have correct asymptotic behavior far from the interface; (ii) to give γ_0 in the limiting case of a flat interface; (iii) to satisfy identically the general thermodynamic relation [14]

$$J(a) + \tfrac{1}{2}a\,\frac{\mathrm{d}J(a)}{\mathrm{d}a} = \sigma(a) - a\,\frac{\mathrm{d}\sigma(a)}{\mathrm{d}a} \tag{1.10}$$

(with $\sigma(a)$ and $J(a)$ being defined through Eqns (1.8) and (1.9)).

The curvature dependence of σ and J can be presented in the form of asymptotic expansions [14]

$$\sigma(\epsilon)=\sum_{n=0}^{\infty}\sigma_n g_n(\epsilon) \qquad J(\epsilon)=\sum_{n=0}^{\infty}J_n g_n(\epsilon) \tag{1.11}$$

where the small parameter is

$$\epsilon=b/a \tag{1.12}$$

b is a parameter with a dimension of length, characterizing the width of the interfacial transition region. σ_n and J_n are coefficients, and $g_n(\epsilon)$, $n=0,1,2,...$ is an asymptotic sequence of gauge functions (see Ref. [22] for the theory of asymptotic expansions).

It is demonstrated in Section 2 below that the knowledge of the asymptotic behavior of $\Delta P(r,a)$ far from the interface allows determination of the gauge functions $g_n(\epsilon)$, $n=0, 1,2,....$ Connections between the coefficient functions σ_n and J_n, arising from Eqn (1.10), are derived in Section 3. A model expression for the behavior of $\Delta P(r,a)$ close to the interfacial transition region is proposed in Section 4 and the parameters of the model are determined by using the conditions (i)–(iii) formulated above. The equations derived for the calculation of δ_0, B_0, $\sigma(a)$, $\gamma(a)$, $B(a)$ etc. are summarized in Section 5. Section 6 presents numerical data calculated by means of our model for different interfaces: liquid argon–gas, water–gas, liquid benzene–gas, paraffin hydrocarbons–gas, benzene–water and paraffin hydrocarbons–water. The results are discussed and summarized in Section 7.

2. CONTRIBUTION OF THE "TAILS" OF $\Delta P(r,a)$ TO THE INTERFACIAL TENSION

The definition domain of the function $\Delta P=\Delta P(r)$ can be divided into three parts: an inner region at $a-b\leqslant r\leqslant a+b$ where the anisotropy of the pressure tensor is well pronounced and two outer regions, I and II, where the anisotropy ΔP vanishes with the increase in the distance to the interface (see Fig. 1). (The physical background for the introduction of these three regions is discussed in Section 3 of Part I [14].) The parameter b, characterizing the width of the inner region, is a parameter of our model liable to determination (see below). Let us denote by $\Delta P^{in}(r,a)$, $\Delta P^{I}(r,a)$ and $\Delta P^{II}(r,a)$ the values of $\Delta P(r,a)$ in the inner and in the respective two outer regions I and II. In Part 1 of this study [14] we derived asymptotic expressions for $\Delta P^{I}(r,a)$ and $\Delta P^{II}(r,a)$ (Eqns (5.5) and (6.5) respectively in Ref. [14]).

Having in mind Eqns (1.8) and (1.9), one can write [14]

$$\sigma=\sigma^{I}+\sigma^{in}+\sigma^{II} \tag{2.1}$$

$$J=J^{I}+J^{in}+J^{II} \tag{2.2}$$

where

$$\sigma^{\mathrm{I}}=\int_0^{a-b}\Delta P^{\mathrm{I}}(r,a)\frac{a}{r}\,\mathrm{d}r \qquad \sigma^{\mathrm{II}}=\int_{a+b}^{\infty}\Delta P^{\mathrm{II}}(r,a)\frac{a}{r}\,\mathrm{d}r \tag{2.3}$$

$$J^{\mathrm{I}}=\int_0^{a-b}\Delta P^{\mathrm{I}}(r,a)\frac{r^2}{a^2}\,\mathrm{d}r \qquad J^{\mathrm{II}}=\int_{a+b}^{\infty}\Delta P^{\mathrm{II}}(r,a)\frac{r^2}{a^2}\,\mathrm{d}r \tag{2.4}$$

$$\sigma^{\mathrm{in}}=\int_{a-b}^{a+b}\Delta P^{\mathrm{in}}(r,a)\frac{a}{r}\,\mathrm{d}r \qquad J^{\mathrm{in}}=\int_{a-b}^{a+b}\Delta P^{\mathrm{in}}(r,a)\frac{r^2}{a^2}\,\mathrm{d}r \tag{2.5}$$

In view of Eqn (2.1), one can conclude that σ^{I} and σ^{II} represent the contributions of the two outer regions to the value of the interfacial tension σ. Explicit expressions for σ^{I} and σ^{II} can be obtained by substitution of the asymptotic expressions for $\Delta P^{\mathrm{I}}(r,a)$ and $\Delta P^{\mathrm{II}}(r,a)$ (Eqns (5.5) and (6.5) of Part 1 [14]) into Eqn (2.3) and by carrying out the integration. In accordance with Eqn (1.12) the results are

$$\sigma^{\mathrm{I}}(\epsilon)=-\frac{\epsilon^2}{8\pi b^2}\left\{\frac{A}{2}\left[\frac{1}{(1-\epsilon)^2}+\frac{1}{3}-\frac{1}{2(1-\epsilon)^3}\ln\frac{2-\epsilon}{\epsilon}\right.\right.$$
$$\left.\left.-A_1\left[\frac{2+2\epsilon-\epsilon^2}{(2-\epsilon)^2\epsilon^2}+\frac{1}{(1-\epsilon)^2}-\frac{8}{3}-\frac{1}{2(1-\epsilon)^3}\ln\frac{2-\epsilon}{\epsilon}\right]\right\} \tag{2.6}$$

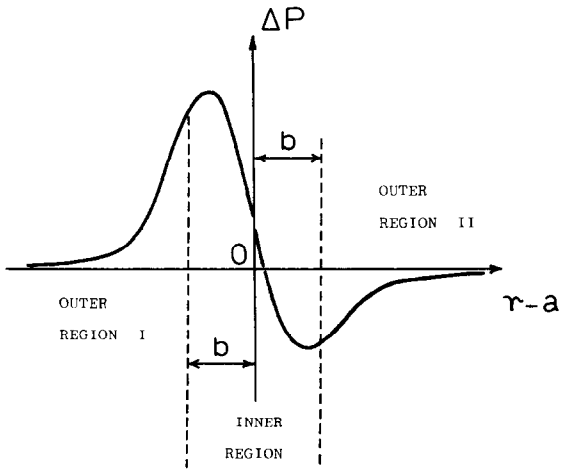

Fig. 1. Sketch of the anisotropy of the pressure tensor distribution, $\Delta P=P_{\mathrm{N}}-P_{\mathrm{T}}$, as a function of the distance to the equimolecular dividing surface, in a system of two neighboring fluid phases; b represents the half-width of the transition region.

$$\sigma^{II}(\epsilon)=\frac{\Lambda_2}{8\pi b^2}\left[\frac{2-2\epsilon-\epsilon^2}{(2+\epsilon)^2}+\frac{\epsilon^2}{(1+\epsilon)^2}-\frac{\epsilon^2}{2(1+\epsilon)^3}\ln\frac{2+\epsilon}{\epsilon}\right] \tag{2.7}$$

Here

$$A=\Lambda_1+\Lambda_2 \tag{2.8}$$

with

$$\Lambda_1=\pi^2(\alpha_{11}\rho_1^2-\alpha_{12}\rho_1\rho_2) \tag{2.9}$$

$$\Lambda_2=\pi^2(\alpha_{22}\rho_2^2-\alpha_{12}\rho_1\rho_2) \tag{2.10}$$

ρ_1 and ρ_2 are the number densities in the bulk of the two phases I and II and α_{ij} $(i,j=1,2)$ are the constants taking part in the expression $\phi_{ij}(R)=-\alpha_{ij}/R^6$ for the potential energy of van der Waals interaction between a molecule from component i and a molecule from component j separated at a distance R. In fact A in Eqn (2.8) is the known Hamaker constant characterizing the van der Waals interaction between the two neighboring phases [23,24].

The analogous expressions for J^I and J^{II} follow after substitution of the asymptotic expressions for $\Delta P^I(r,a)$ and $\Delta P^{II}(r,a)$ (Eqns (5.5) and (6.5) of Part 1) into Eqn (2.4) and carrying out the integration:

$$J^I(\epsilon)=-\frac{\epsilon^2}{8\pi b^2}\left\{\frac{A}{2}\left[3\Phi(1-\epsilon)-2(1-\epsilon)-\frac{1}{2}\ln\frac{2-\epsilon}{\epsilon}\right]\right.$$
$$\left.-\Lambda_1\left[\frac{2(1-\epsilon)(1-4\epsilon+2\epsilon^2)}{(2-\epsilon)^2\epsilon^2}+3\Phi(1-\epsilon)-\frac{1}{2}\ln\frac{2-\epsilon}{\epsilon}\right]\right\} \tag{2.11}$$

and

$$J^{II}(\epsilon)=\frac{\epsilon^2}{8\pi b^2}\Lambda_2\left[\frac{2(1+\epsilon)(1+4\epsilon+2\epsilon^2)}{(2-\epsilon)^2\epsilon^2}-3\Phi\left(\frac{1}{1+\epsilon}\right)-\frac{1}{2}\ln\frac{2+\epsilon}{\epsilon}\right] \tag{2.12}$$

where we have used the notation

$$\Phi(x)=\int_0^x \operatorname{arc\,tanh} y\,\frac{dy}{y}=\sum_{n=0}^{\infty}\frac{x^{2n+1}}{(2n+1)^2} \qquad x\leqslant 1 \tag{2.13}$$

It is worthwhile noting that

$$\Phi(1)=\pi^2/8 \tag{2.14}$$

As mentioned above, ϵ is a small parameter and one can represent Eqns (2.6), (2.7), (2.11) and (2.12) in the form of asymptotic expansions for $\epsilon\ll 1$:

$$\sigma^Y(\epsilon)=\sigma_0^Y+\sigma_1^Y\epsilon+\sigma_2^Y\epsilon^2\ln\epsilon+\sigma_3^Y\epsilon^2+O(\epsilon^3\ln\epsilon) \tag{2.15}$$

$$J^Y(\epsilon)=J_0^Y+J_1^Y\epsilon+J_2^Y\epsilon^2\ln\epsilon+J_3^Y\epsilon^2+O(\epsilon^3\ln\epsilon) \quad Y=I,\,II. \tag{2.16}$$

TABLE 1

The coefficients in the expansions (2.15) and (2.16), calculated from Eqns (2.6), (2.7), (2.11) and (2.12)

k	σ_k^{I}	σ_k^{II}	J_k^{I}	J_k^{II}
0	$\eta\Lambda_1$	$\eta\Lambda_2$	$\eta\Lambda_1$	$\eta\Lambda_2$
1	$2\eta\Lambda_1$	$-2\eta\Lambda_2$	$-4\eta\Lambda_1$	$-4\eta\Lambda_2$
2	$-\frac{1}{2}\eta(A-2\Lambda_1)$	$\eta\Lambda_2$	$\frac{1}{2}\eta(A-2\Lambda_1)$	$\eta\Lambda_2$
3	$-\eta\Lambda_1(\ln 2+\frac{25}{12})$ $+\eta A(\frac{1}{2}\ln 2-\frac{4}{3})$	$-\eta\Lambda_2(\ln 2-\frac{13}{4})$	$-\eta\Lambda_1(\ln 2-\frac{7}{4}+\frac{3}{4}\pi^2)+$ $+\frac{\eta}{2}A(\ln 2+4-\frac{1}{4}\pi^2)$	$-\eta\Lambda_2(\ln 2-\frac{7}{4}+\frac{1}{4}\pi^2)$

The coefficients σ_k^{Y} and J_k^{Y} (Y=I,II), calculated from Eqns (2.6), (2.7) and (2.11)–(2.14) are presented in Table 1 for $k=0,1,2$ and 3. For the sake of brevity we have used the notation

$$\eta=1/(16\pi b^2) \tag{2.17}$$

Equations (2.15) and (2.16) show that the four functions $\sigma^{\mathrm{I}}(\epsilon)$, $\sigma^{\mathrm{II}}(\epsilon)$, $J^{\mathrm{I}}(\epsilon)$ and $J^{\mathrm{II}}(\epsilon)$ have asymptotic expansions in terms of one and the same asymptotic sequence of gauge functions:

$$1,\ \epsilon,\ \epsilon^2\ln\epsilon,\ \epsilon^2,\ \epsilon^3\ln\epsilon,\ \epsilon^3,\ \ldots \tag{2.18}$$

So, we think it is reliable to identify the gauge functions $g_n(\epsilon)$, $n=0,1,2,\ldots$, in Eqn (1.11) with the sequence (2.18). In other words, we will seek $\sigma(\epsilon)$ and $J(\epsilon)$ in the form

$$\sigma(\epsilon)=\sigma_0+\sigma_1\epsilon+\sigma_2\epsilon^2\ln\epsilon+\sigma_3\epsilon^2+O(\epsilon^3\ln\epsilon) \tag{2.19}$$

$$J(\epsilon)=J_0+J_1\epsilon+J_2\epsilon^2\ln\epsilon+J_3\epsilon^2+O(\epsilon^3\ln\epsilon) \tag{2.20}$$

Equation (1.10) provides connections between coefficients σ_k and J_k, $k=0,1,2,\ldots$, in Eqns (2.19) and (2.20) which are studied below.

3. CONNECTIONS BETWEEN THE COEFFICIENTS σ_k AND J_k

By means of Eqn (1.12) one can transform Eqn (1.10) to read

$$\sigma(\epsilon)+\epsilon\frac{\mathrm{d}\sigma(\epsilon)}{\mathrm{d}\epsilon}=J(\epsilon)-\tfrac{1}{2}\epsilon\frac{\mathrm{d}J(\epsilon)}{\mathrm{d}\epsilon} \tag{3.1}$$

Equations (2.19) and (2.20) yield

$$\sigma+\epsilon\frac{\mathrm{d}\sigma}{\mathrm{d}\epsilon}=\sigma_0+2\sigma_1\epsilon+3\sigma_2\epsilon^2\ln\epsilon+(\sigma_2+3\sigma_3)\epsilon^2+\ldots \tag{3.2}$$

$$J-\frac{\epsilon}{2}\frac{\mathrm{d}J}{\mathrm{d}\epsilon}=J_0+\tfrac{1}{2}J_1\epsilon-\tfrac{1}{2}J_2\epsilon^2+\ldots \tag{3.3}$$

In accordance with Eqn (3.1), the coefficients multiplying the identical gauge functions in Eqns (3.2) and (3.3) must be equal. Thus one finds

$$\sigma_0=J_0 \tag{3.4}$$

$$2\sigma_1=\tfrac{1}{2}J_1 \tag{3.5}$$

$$\sigma_2=0 \tag{3.6}$$

$$3\sigma_3=-\tfrac{1}{2}J_2 \tag{3.7}$$

etc. Equation (3.4) is trivial because it does not lead to any restriction on the function $\Delta P(r,a)$. Indeed, by introducing a new integration variable $z=r-a$ in Eqn (1.8) one obtains

$$\sigma_0=\lim_{1/a\to 0}\int_{-a}^{\infty}\Delta P\frac{\mathrm{d}z}{1+\frac{z}{a}}=\int_{-\infty}^{\infty}\Delta P|_{1/a=0}\,\mathrm{d}z=\gamma_0 \tag{3.8}$$

Similarly, Eqn (1.9) yields

$$J_0=\lim_{1/a\to 0}\int_{-a}^{\infty}\Delta P\left(1+\frac{z}{a}\right)^2\mathrm{d}z=\int_{-\infty}^{\infty}\Delta P|_{1/a=0}\,\mathrm{d}z=\sigma_0 \tag{3.9}$$

In other words, $\sigma_0=J_0$ only if ΔP tends to zero far from the interface fast enough to guarantee convergency of the integrals in Eqns (3.8) and (3.9). However, the other conditions (3.5), (3.6), (3.7) etc. are not trivial. Each of these allows determination of one unknown parameter of the model. In the next section we will use this fact to determine the dependence of $\Delta P^{\mathrm{in}}(r,a)$ on a.

Let us now compare Eqn (2.19) with the Gibbs–Tolman equation [Eqn (1.6)]. In view of Eqn (1.12) and by comparing the coefficients at ϵ^1 one obtains

$$\sigma_1=-\sigma_0\,\delta_0/b \tag{3.10}$$

Alternatively, by substituting from Eqns (1.3) and (1.6) into Eqn (1.7) one derives

$$J=\sigma_0\left[1-\frac{4\delta_0}{a}+o\left(\frac{1}{a}\right)\right] \tag{3.11}$$

(cf. also Eqn (1.2)). Then the comparison of Eqns (2.20) and (3.11) yields

$$J_1=-4\,\sigma_0\,\delta_0/b \tag{3.12}$$

From Eqns (3.10) and (3.12) it follows that $J_1=4\sigma_1$, which means that Eqn

(3.5) is in agreement with the Gibbs–Tolman formula. Besides, if we determine b and σ_1 (or J_1) in the framework of our model, Eqns (1.4) and (3.10) provide formulae for calculation of δ_0 and B_0:

$$\sigma_0 = -\sigma_1 b/\sigma_0 \qquad B_0 = -2\sigma_1 b \tag{3.13}$$

In addition, it follows from Eqns (2.1), (2.15) and (2.19) that

$$\sigma^{\text{in}}(\epsilon) = \sigma_0^{\text{in}} + \sigma_1^{\text{in}}\epsilon + \sigma_2^{\text{in}}\epsilon^2 \ln \epsilon + \sigma_3^{\text{in}}\epsilon^2 + O(\epsilon^3 \ln \epsilon) \tag{3.14}$$

where by definition

$$\sigma_k^{\text{in}} = \sigma_k - \sigma_k^{\text{I}} - \sigma_k^{\text{II}} \qquad k=0, 1, 2,... \tag{3.15}$$

Analogously, from Eqns (2.2), (2.16) and (2.20) one obtains

$$J^{\text{in}}(\epsilon) = J_0^{\text{in}} + J_1^{\text{in}}\epsilon + J_2^{\text{in}}\epsilon^2 \ln \epsilon + J_3^{\text{in}}\epsilon^2 + O(\epsilon^3 \ln \epsilon) \tag{3.16}$$

with

$$J_k^{\text{in}} = J_k - J_k^{\text{I}} - J_k^{\text{II}} \qquad k=0, 1, 2,... \tag{3.17}$$

We will make use of these equations in the next section.

4. MODEL EXPRESSION FOR $\Delta P^{\text{in}}(r,a)$

From the viewpoint of statistical mechanics, ΔP^{in} depends on the short-range interactions in the interfacial zone. For that reason the calculation of ΔP^{in} from first principles is a difficult problem. This problem has been solved for simple liquids by means of some quasi-thermodynamic simplifications and/or by means of computer solution of some integral equations of statistical mechanics [10,12,25,26].

Since we are interested in some interfacial properties expressed through integrals over ΔP^{in}, we propose here an alternative semiempirical model approach for determining $\Delta P^{\text{in}}(r,a)$. It is based on a series of some general restrictions imposed on the function $\Delta P^{\text{in}}(r,a)$. The first restriction originates from Eqn (3.8), where the tension γ_0 of the flat interface is supposed to be known from experiment. By means of Eqns (1.2), (2.5), (2.15) and (3.15) the expression (1.8) can be transformed to read

$$\sigma_0^{\text{in}} = \lim_{1/a \to 0} \int_{a-b}^{a+b} \Delta P^{\text{in}}(a,r)\, \frac{a}{r}\, \mathrm{d}r = \gamma_0 - \sigma_0^{\text{I}} - \sigma_0^{\text{II}} \tag{4.1}$$

Values of σ_0^{I} and σ_0^{II} are given in Table 1. The second restriction is a natural condition for smooth matching of $\Delta P^{\text{in}}(r,a)$ with $\Delta P^{\text{I}}(r,a)$ and $\Delta P^{\text{II}}(r,a)$ at the boundaries of the inner region. This condition leads to the following equations:

$$\Delta P^{\text{in}}(a-b,a) = \Delta P^{\text{I}}(a-b,a) = p_1(a) \tag{4.2}$$

$$\Delta P^{\text{in}}(a+b,a)=\Delta P^{\text{II}}(a+b,a)=p_2(a) \tag{4.3}$$

$$\left.\frac{\partial \Delta P^{\text{in}}}{\partial r}\right|_{r=a-b}=\left.\frac{\partial \Delta P^{\text{I}}}{\partial r}\right|_{r=a-b}=q_1(a) \tag{4.4}$$

$$\left.\frac{\partial \Delta P^{\text{in}}}{\partial r}\right|_{r=a+b}=\left.\frac{\partial \Delta P^{\text{II}}}{\partial r}\right|_{r=a+b}=q_2(a) \tag{4.5}$$

It should be noted that $p_1(a), p_2(a), q_1(a)$ and $q_2(a)$ can easily be determined from the known asymptotics for $\Delta P^{\text{I}}(r,a)$ and $\Delta P^{\text{II}}(r,a)$ (Eqns (5.5) and (6.5) of Part 1 [14]).

The third restriction states that $\Delta P^{\text{in}}(r,a)$ must satisfy Eqns (3.14) and (3.16) whose left-hand sides are given by Eqn (2.5). This restriction concerns the dependence of ΔP^{in} on a.

The fourth restriction implies that Eqns (3.5), (3.6), (3.7) etc. must be satisfied. Owing to Eqns (3.15), (3.17) and Table 1, this restriction leads to some conditions for σ_k^{in} and J_k^{in} $(k=1,2,3,\ldots)$, which in turn are connected with $\Delta P^{\text{in}}(r,a)$ (cf. Eqns (2.5), (3.14) and (3.16)).

Below we will propose an appropriate expression for ΔP^{in} containing several parameters which are intended to be determined from the restrictions enumerated above. In the inner region, $a-b\leqslant r\leqslant a+b$, it is convenient to replace r with the dimensionless variable

$$\xi=\frac{1}{2b}(r-a+b) \tag{4.6}$$

The boundary points $r=a-b$ and $r=a+b$ correspond to $\xi=0$ and $\xi=1$ respectively. Let us consider the model expression

$$\Delta P^{\text{in}}=c_0+c_1\xi+c_2\xi^2+c_3\xi^3+f(\epsilon)(p_1+p_2)\xi^2(1-\xi)^2 \tag{4.7}$$

where

$$f(\epsilon)=\lambda_0\epsilon+\lambda_1\epsilon^2\ln\epsilon+\lambda_2\epsilon^2+\ldots \tag{4.8}$$

and $\lambda_0, \lambda_1, \lambda_2, \ldots$, are constant parameters. For a flat interface $(\epsilon=0)$ the last term in Eqn (4.7) disappears and ΔP^{in} reduces to a cubic parabola; this simple curve in principle can have a minimum and a maximum, as is expected for ΔP in the inner region (see Fig. 1).

Obviously the last term in Eqn (4.7) and its derivative with respect to ξ are zero at the boundary points $\xi=0$ and $\xi=1$. Hence the four parameters c_0, c_1, c_2 and c_3 can be determined in terms of p_1, p_2, q_1 and q_2 by means of the four conditions [Eqns (4.2) – (4.5)]. In this way Eqn (4.7) can be transformed to read

$$\Delta P^{\text{in}} = p_1(1-\xi) + p_2\xi + (p_1 - p_2 + 2bq_1)\xi(1-\xi)^2 + (p_2 - p_1 - 2bq_2)\xi^2(1-\xi) + f(\epsilon)(p_1+p_2)\xi^2(1-\xi)^2 \tag{4.9}$$

The expansion in terms of the asymptotic sequence (2.18) in Eqn (4.8) was introduced to provide agreement of Eqn (4.7) with Eqns (3.14) and (3.16). Besides, the parameters $\lambda_0, \lambda_1, \lambda_2$ etc. are to be determined in such a way that Eqns (3.5), (3.6), (3.7) etc. be satisfied. With this end in view, let us first determine the coefficients σ_k^{in} and J_k^{in} in Eqns (3.14) and (3.16) by means of Eqn (4.9).

According to Eqn (1.12) the parameters p_1, p_2, q_1 and q_2 in Eqn (4.9) depend on ϵ. From Eqns (4.2)–(4.5) one derives

$$p_k(\epsilon) = p_{k0} + p_{k2}\,\epsilon^2 + O(\epsilon^3 \ln \epsilon) \qquad k=1,2 \tag{4.10}$$

$$q_k(\epsilon) = q_{k0} + q_{k2}\,\epsilon^2 + O(\epsilon^3) \qquad k=1,2 \tag{4.11}$$

where

$$p_{k0} = (-1)^{k+1}\frac{b}{3}\,q_{k0} = \frac{\Lambda_k}{8\pi b^3} \tag{4.12}$$

$$p_{12} = bq_{12} = \frac{A - 6\Lambda_1}{32\pi b^3} \tag{4.13}$$

$$p_{22} = -bq_{22} = -\frac{3\Lambda_2}{16\pi b^3} \tag{4.14}$$

Λ_1, Λ_2 and A are defined by Eqns (2.8)–(2.10). By substitution of Eqn (4.9) in Eqn (2.5), after some calculations, one obtains the following expressions for the coefficients σ_k^{in} and J_k^{in}:

$$\sigma_0^{\text{in}} = J_0^{\text{in}} = b(p_{10}+p_{20}) + \frac{b^2}{3}(q_{10} - q_{20}) \tag{4.15}$$

$$\begin{aligned}\sigma_1^{\text{in}} &= -\tfrac{1}{2}J_1^{\text{in}} + \lambda_0\frac{b}{10}(p_{10}+p_{20}) \\ &= \frac{2b}{5}(p_{10}-p_{20}) + \frac{b^2}{15}(q_{10}+q_{20}) + \lambda_0\frac{b}{15}(p_{10}+p_{20})\end{aligned} \tag{4.16}$$

$$\sigma_2^{\text{in}} = J_2^{\text{in}} = \lambda_1\frac{b}{15}(p_{10}+p_{20}) \tag{4.17}$$

$$\begin{aligned}\sigma_3^{\text{in}} = J_3^{\text{in}} &= \frac{b}{3}(p_{10}+p_{20}) + b(p_{12}+p_{22}) \\ &\quad + \frac{b^2}{15}(q_{10}-q_{20}) + \frac{b^2}{3}(q_{12}-q_{22}) + \lambda_2\frac{b}{15}(p_{10}+p_{20})\end{aligned} \tag{4.18}$$

Now we are ready to determine the parameters of the model, namely, b, λ_0, λ_1 and λ_2. A substitution from Eqn (4.15) and Table 1 into Eqn. (4.1), along with Eqns (2.8)–(2.10) and (4.12), yields

$$\gamma_0 = \frac{5}{16\pi}\frac{A}{b^2} \tag{4.19}$$

This simple relation determines b at a known interfacial tension of the flat interface γ_0 and Hamaker constant A. From Eqns (3.5), (3.15) and (3.17) one derives

$$4(\sigma_1^{\mathrm{I}} + \sigma_1^{\mathrm{II}} + \sigma_1^{\mathrm{in}}) = J_1^{\mathrm{I}} + J_1^{\mathrm{II}} + J_1^{\mathrm{in}} \tag{4.20}$$

Then a substitution from Table 1 and Eqn (4.16) into Eqn (4.20) leads to

$$\lambda_0 = 48\frac{\Lambda_2 - \Lambda_1}{A} \tag{4.21}$$

In addition, from Eqns (3.6) and (3.15) one derives

$$\sigma_2^{\mathrm{I}} + \sigma_2^{\mathrm{II}} + \sigma_2^{\mathrm{in}} = 0 \tag{4.22}$$

In accordance with Eqn (4.17) and Table 1, Eqn (4.22) yields

$$\lambda_1 = -\frac{15}{4} \tag{4.23}$$

Finally, in view of Eqns (3.15) and (3.17) one transforms Eqn (3.7) to read

$$-6\,(\sigma_3^{\mathrm{I}} + \sigma_3^{\mathrm{II}} + \sigma_3^{\mathrm{in}}) = J_2^{\mathrm{I}} + J_2^{\mathrm{II}} + J_2^{\mathrm{in}} \tag{4.24}$$

By substitution from Eqns (4.17), (4.18), (4.23) and Table 1 in Eqn (4.24), one obtains

$$\lambda_2 = \frac{3}{8}(10\ln 2 + 7) + 40\frac{\Lambda_1}{A} \tag{4.25}$$

It should be noted that in principle the expansion (4.8) can be continued and in a similar way the next coefficients λ_3, λ_4,... can be determined by means of the next members of the family of Eqns. (3.4)–(3.7). However, the first three terms in Eqn (4.8) are enough to provide a good numerical consistence of our model with the general thermodynamic condition [Eqn (3.1)]. The physical consistence of the model can be checked by comparing its predictions with experiment and with the available numerical data. This is done in Section 6 below.

5. CALCULATION PROCEDURE

In this section, on the basis of the above results, we will consider the proce-

dures for calculating the different interfacial properties: the mechanical and thermodynamical interfacial tensions $\sigma(a)$ and $\gamma(a)$, the interfacial bending moment $B(a)$, the Gibbs–Tolman parameter δ_0, the profile of $\Delta P(r,a)$ etc.

First, we recall that all interfacial properties of a spherical interface, considered in the present paper, are related to the equimolecular dividing surface of radius a, defined in such a way that the adsorption of component 1 (inside the drop/bubble) be zero. Their values for other dividing surfaces can be calculated by using standard thermodynamic relations (see for example Refs [19,20,27]). In particular, the questions about the definition of the interfacial bending moment B and about its dependence on the choice of the dividing surface (as well as about the difference between σ and γ) are considered in detail in Ref. [15].

We will suppose that the interfacial tension of the flat interface, $\gamma_0=\sigma_0$, as well as the constants of the van der Waals interaction A_1, A_2 and A are known. A_1 and A_2 are defined by Eqns (2.9) and (2.10), and $A=A_1+A_2$ (cf. Eqn (2.8)).

By using the values of γ_0, A, A_1 and A_2 one can calculate the parameters of the model: b from Eqn (4.19), λ_0 from Eqn (4.21) and λ_2 from Eqn (4.25); λ_1 is always equal to $-15/4$ in the framework of this model. It should be noted that both λ_0 and λ_2 depend on which component (1 or 2) is inside the drop (bubble) and which one is outside. Then one can proceed with calculation of the curvature dependence of the interfacial tension.

5.1 Parameters in the Gibbs–Tolman equation

The approximate Gibbs–Tolman equation in its forms (1.3), (1.5) or (1.6) can be used for calculation of the curvature dependence of interfacial tension if only the value of the parameter δ_0 (or B_0) is available. In our model, δ_0 and B_0 can be determined from the value of the coefficient σ_1 by using Eqn (3.13). According to Eqn (3.15)

$$\sigma_1=\sigma_1^{\mathrm{I}}+\sigma_1^{\mathrm{II}}+\sigma_1^{\mathrm{in}} \tag{5.1}$$

If one substitutes for σ_1^{I} and σ_1^{II} from Table 1 and for σ_1^{in} from Eqn (4.16), then Eqn (5.1) along with Eqns (2.8) and (4.10)–(4.14) yields

$$\sigma_1=\frac{A_2-A_1}{5\pi b^2} \tag{5.2}$$

Then a substitution from Eqn (5.2) into Eqn (3.13) yields

$$\delta_0=\frac{A_1-A_2}{5\pi b\,\gamma_0} \tag{5.3}$$

$$B_0=\frac{2(A_1-A_2)}{5\pi b} \tag{5.4}$$

The numerical results, presented in the next section, show that the Gibbs–Tolman equation accounts with good accuracy for the curvature dependence of the interfacial tension, the higher-order terms being usually negligible. In addition, it turns out that $B(a) \approx B_0 = \text{constant}$.

5.2 Higher-order terms in the curvature dependence of σ

For the time being the higher-order curvature effects (the terms neglected in Eqns (1.3), (1.5) or (1.6)) are under the threshold of experimental accuracy. In spite of that, the question as to what is the next term in the Gibbs–Tolman equation (proportional to ϵ^2 or to $\epsilon^2 \ln \epsilon$) represents independent interest. Our model provides expressions for the higher-order terms. Of course, we are conscious of the fact that the model simplifications used can cast some doubt on the reliability of these expressions. Nevertheless, in as far as the general thermodynamic condition, Eqn (1.10), was utilized, we will discuss briefly the higher-order terms.

Equation (3.6), which is a corollary from the general equation, Eqn (1.10), states that $\sigma_2 = 0$, i.e. the term proportional to $\epsilon^2 \ln \epsilon$ in Eqn (2.19) is zero. One can check that J_2 is also zero. Indeed, it follows from Eqn (3.17) that

$$J_2 = J_2^{\mathrm{I}} + J_2^{\mathrm{II}} + J_2^{\mathrm{in}} \tag{5.5}$$

The substitution of J_2^{I} and J_2^{II} from Table I and of J_2^{in} from Eqn (4.17) into Eqn (5.5) leads to

$$J_2 = 0 \tag{5.6}$$

In other words, the term proportional to $\epsilon^2 \ln \epsilon$ in Eqn (2.20) turns out to be zero too. Further, a combination of Eqn (3.7), which is also a corollary from Eqn (1.10), with Eqn (5.6) yields

$$\sigma_3 = 0 \tag{5.7}$$

However, J_3 is not zero. From Eqns (3.17), (4.18), (4.25) and Table 1 one derives

$$J_3 = \frac{1}{16\pi b^2}\left[A\left(\frac{11}{6} - \frac{9}{8}\pi^2\right) + \frac{16}{3}\Lambda_1\right] \tag{5.8}$$

In view of these results, Eqn (2.19) takes the form

$$\sigma(a) = \sigma_0 + \sigma_1 \frac{b}{a} + o\left(\frac{b^2}{a^2}\right) \tag{5.9}$$

where σ_1 is given by Eqn (5.2), and Eqns (1.12) and (3.8) are also used. According to Eqn (3.13) the formula (5.9) confirms the validity of Eqn (1.6), where the first neglected term turns out to be of an order higher than b^2/a^2 (see the note after Eqn. (1.5)).

Equations (2.20), (3.5), (3.9) and (5.6) yield a counterpart of Eqn (5.9) for $J(a)$:

$$J(a)=\sigma_0+4\sigma_1\frac{b}{a}+J_3\frac{b^2}{a^2}+o\left(\frac{b^2}{a^2}\right) \tag{5.10}$$

where σ_1 and J_3 can be calculated from Eqns (5.2) and (5.8). By substitution from Eqns (5.9) and (5.10) into Eqn (1.7), along with Eqn (1.2), one obtains a generalization of the classical Gibbs–Tolman formula [Eqn (1.3)]:

$$\gamma(a)=\gamma_0+2\sigma_1\frac{b}{a}+\tfrac{1}{3}J_3\frac{b^2}{a^2}+o\left(\frac{b^2}{a^2}\right) \tag{5.11}$$

Besides, by means of Eqns (1.1), (1.2), (3.13), (5.9) and (5.11) one derives an equation for the curvature dependence of B:

$$B(a)=B_0-(\tfrac{2}{3}\,b\,J_3)\frac{b}{a}+o\left(\frac{b}{a}\right) \tag{5.12}$$

where B_0 and J_3 are to be calculated from Eqns (5.4) and (5.8).

5.3 Calculation of $\Delta P(r,a)$

$\Delta P=P_N-P_T$ expresses the anisotropy of the pressure tensor due to the interfacial forces. In our model, ΔP is represented in the form

$$\Delta P(r,a)=\begin{cases}\Delta P^{I}(r,a) & \text{for } 0\leqslant r<a-b\\ \Delta P^{in}(r,a) & \text{for } a-b\leqslant r\leqslant a+b\\ \Delta P^{II}(r,a) & \text{for } a+b<r<\infty\end{cases} \tag{5.13}$$

where ΔP^{I} and ΔP^{II} are given by Eqns (5.5) and (6.5) of Part 1 [14], ΔP^{in} by Eqn (4.9), and the quantities ϵ and ξ are given by Eqns (1.12) and (4.6). The parameters b, p_1, p_2, q_1, q_2 and $f(\epsilon)$ are expressed through Λ_1, Λ_2 and γ_0 as follows:

$$b=\left(\frac{5A}{16\pi\gamma_0}\right)^{1/2} \tag{5.14}$$

$$p_1=\frac{\Lambda_1}{8\pi b^3}\left(1+\epsilon^2\frac{A-6\Lambda_1}{4\Lambda_1}\right)\qquad p_2=\frac{\Lambda_2}{8\pi b^3}\left(1-\frac{3}{2}\epsilon^2\right) \tag{5.15}$$

$$q_1=\frac{3\Lambda_1}{8\pi b^4}\left(1+\epsilon^2\frac{A-6\Lambda_1}{12\Lambda_1}\right)\qquad q_2=-\frac{3\Lambda_2}{8\pi b^4}\left(1-\frac{1}{2}\epsilon^2\right) \tag{5.16}$$

$$f(\epsilon)=48\,\epsilon\frac{\Lambda_2-\Lambda_1}{A}-\frac{15}{4}\epsilon^2\ln\epsilon+\epsilon^2\left[\frac{3}{8}(7+10\ln 2)+40\frac{\Lambda_1}{A}\right] \tag{5.17}$$

Equations (5.14)–(5.17) can be easily derived from Eqns (4.10)–(4.14), (4.21), (4.23), (4.25). From the expression (5.13) for $\Delta P(r,a)$ one can calculate $P_N(r,a)$ by using the hydrostatic equilibrium condition, Eqn (6.5) (see below). The other component of the pressure tensor, P_T, simply equals $P_N - \Delta P$. In this way one calculates all components of the pressure tensor. According to the procedure used the tensor thus calculated will satisfy the three general physical conditions formulated after Eqn (1.9) in the Introduction.

6. NUMERICAL RESULTS AND DISCUSSION

Our model in its present form is applicable only to interfaces whose surface tension is expected to be due to the surface excess van der Waals interaction. In the case when there are surfactant molecules adsorbed at the interface, our model enables us to calculate the component of the interfacial bending moment, which is due to the van der Waals interactions. (In Ref. [16] this component was denoted B_p).

Below we will first consider liquid/gas interfaces and secondly oil/water interfaces.

6.1 Liquid/gas interfaces

We will suppose that the density of the gas phase is small enough to be set equal to zero ($\rho_2 \approx 0$) in Eqns (2.8)–(2.10). Then one can write

$$A = \Lambda_1 = \pi^2 \alpha_{11} \rho_1^2 \qquad \Lambda_2 = 0 \tag{6.1}$$

ρ_1 is the number density of the component 1 (in this case the liquid phase).

One can calculate the Hamaker constant A in Eqn (6.1) by using data for the parameters ϵ^* and R^* in the Lennard–Jones potential of intermolecular interaction:

$$U(R) = \epsilon^* \left[\left(\frac{R^*}{R} \right)^{12} - 2 \left(\frac{R^*}{R} \right)^{6} \right] \tag{6.2}$$

Then α_{11} in Eqn (6.1) is determined as

$$\alpha_{11} = 2\, \epsilon^*\, (R^*)^6 \tag{6.3}$$

As pointed out in the literature [24,28], a simple integration of the pair interaction energy $U(R)$ in Eqn (6.2) over a liquid phase may lead to inaccurate results because of the non-additive nature of the molecular interactions therein. Below we will use effective values of the interaction parameters ϵ^* and R^*, determined especially for liquids. They differ from the values determined for gases and account for the non-additive interactions still allowing pair summation [11,13,29].

To characterize the mean distance between the centers of two nearest neighboring molecules in the phase I we will use the parameter

$$d_1 = \sqrt[3]{v_1} \tag{6.4}$$

where v_1 is the volume per molecule in the liquid phase. (As discussed below, in the case of liquid paraffins we take for v_1 the volume of a $-CH_2-CH_2-$ fragment.) From a physical viewpoint our model is reliable when the half-width of the transition zone, b, is of the order of d_1.

Let us first consider the interface liquid argon/gas, whose properties have been calculated by means of the methods of statistical mechanics [9,11,13,19]. We determined α_{11} from Eqn (6.3) by using the same values of the parameters ϵ^* and R^* as in the work by Kirkwood and Buff [9]. The resulting value of the Hamaker constant A as well as the experimental value of the surface tension γ_0 at 84.3 K ($-188.85\,^\circ C$) are presented in Table 2. Then we calculated d_1 from Eqn (6.4), b from Eqn (4.19), δ_0 from Eqn (5.3) and B_0 from Eqn (5.4) (cf. also Eqn (6.1)). The results are also shown in Table 2 where the first line is for argon. (The second line corresponds to another choice of values for the Lennard–Jones interaction parameters ϵ^*, R^*, used by other authors (see below)). The calculated value $\delta_0 = 3.8$ Å is in a good agreement with the result of Kirkwood and Buff [9], who obtained $\delta_0 = 3.63$ Å. A quasi-thermodynamic

TABLE 2

Liquid–gas interfaces

Phase I	Temperature (°C)	$A \cdot 10^{20}$ (J)	γ_0 (mN m^{-1})	d_1 (Å)	b (Å)	δ_0 (Å)	$B_0 \cdot 10^{12}$ (N)
Argon	−188.85	4.684[a]	13.45	3.60	5.89	3.77	10.14
		2.213[b]			4.05	2.59	6.97
Water	25	4.500	72.0	3.11	2.49	1.59	22.90
Benzene	20	25.54	28.9	5.28	9.38	6.00	34.68
n-C_5H_{12}	20	8.90	16.1	4.00	7.42	4.75	15.30
n-C_7H_{16}	20	10.66	20.3	3.93	7.23	4.63	18.80
n-C_8H_{18}	20	11.41	21.8	3.91	7.22	4.62	20.14
n-C_9H_{20}	20	11.97	23.0	3.90	7.20	4.61	21.21
n-$C_{10}H_{22}$	20	12.62	23.9	3.89	7.25	4.64	22.18
n-$C_{11}H_{24}$	20	13.08	24.8	3.88	7.24	4.63	22.96
n-$C_{12}H_{26}$	20	13.49	25.5	3.87	7.25	4.64	23.66
n-$C_{13}H_{28}$	20	13.73	26.1	3.87	7.23	4.63	24.17
n-$C_{14}H_{30}$	20	14.19	26.7	3.86	7.27	4.65	24.83
n-$C_{15}H_{32}$	20	14.48	27.2	3.86	7.28	4.66	25.35
n-$C_{16}H_{34}$	20	14.72	27.6	3.85	7.28	4.66	25.72
n-$C_{17}H_{36}$	20	14.97	28.1	3.85	7.28	4.66	26.19

[a]The Lennard–Jones parameters ϵ^*, R^* taken from Ref. [33].
[b]The Lennard–Jones parameters ϵ^*, R^* taken from Ref. [13].

study by Hill [10] gave $\delta_0 = 2.8$ Å, but the surface tension, calculated in the same work, exhibited large deviations from the experimentally determined value at the argon/gas interface (Hill's estimate is $\gamma_0 = 6.0$ mN m^{-1} against the experimental value of 13.45 mN m^{-1} (cf. Table 2)). From molecular dynamics simulations, values for δ_0 were obtained varying in the range 1.5–5.8 Å [26,29,30]. At present it seems to be commonly accepted that for liquid/gas interfaces (not only for argon) the parameter δ_0 should be positive and of the order of a few ångstroms. An exception are the results of Refs [31,32], where negative δ_0 values were obtained by means of the simplified penetrable spheres model.

By using Eqn (5.13) we calculated $\Delta P = P_N - P_T$ for a flat argon/gas interface ($T = 84.3$ K). The resulting curve is compared in Fig. 2 with the respective curve, calculated by Croxton and Ferrier [13]. In our calculations we used the same parameters ϵ^* and R^* as in Ref. [13] (see the second line for argon in Table 2). They yield a value of $2.21 \cdot 10^{-20}$ J for the Hamaker constant A. The zero on the abscissa in Fig. 2 corresponds to the position of the equimolecular dividing surface. One sees that the curve resulting from our model agrees well with the curve calculated by Croxton and Ferrier [13] by means of a statistical mechanical approach. (It is worthwhile noting that the value of γ_0 calculated by Croxton and Ferrier is in excellent agreement with experiment.) In addition, ΔP calculated by using our model exhibits correct asymptotic behavior far from the interface.

The molecular dynamics simulations of the argon/gas interface [26,29] provide ΔP profiles of the same kind as those in Fig. 2. The results of some authors, based on the density gradient theory, indicate that ΔP can be negative on the gas side of a liquid/gas interface [12,25]. However, the molecular dynamics results [26] demonstrate that such an effect is negligible at least for not too high gas densities.

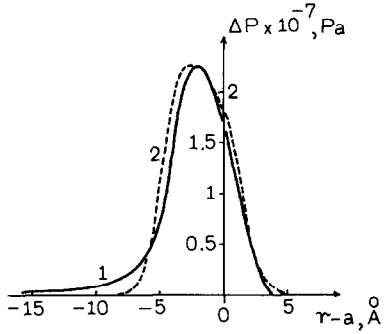

Fig. 2. Anisotropy of the pressure tensor distribution ΔP as a function of the distance to the equimolecular dividing surface for a flat liquid argon/gas interface at 84.3 K: curve 1, according to Eqn (5.13), curve 2, results of Croxton and Ferrier [13].

We also determined the normal pressure component distribution $P_N(r,a)$ by making use of the mechanical equilibrium condition in a fluid system of spherical symmetry [34]:

$$\frac{dP_N}{dr} = -\frac{2}{r}(P_N - P_T) \tag{6.5}$$

On integrating Eqn (6.5) one derives

$$P_N(r,a) - P^{II} = 2\int_r^\infty \Delta P(r,a)\frac{dr}{r} \tag{6.6}$$

where as usual $\Delta P = P_N - P_T$, and P^{II} is the bulk pressure in the outer phase. In view of Eqns (2.3) and (2.5) the normal pressure distribution can be obtained as follows.

(i) For $r > a+b$ (outer region II):

$$P_N(r,a) - P^{II} = 2\int_r^\infty \Delta P\frac{dr}{r} \tag{6.7}$$

(ii) For $a-b < r < a+b$ (inner region):

$$P_N(r,a) - P^{II} = \frac{2}{a}\left[\sigma^{II}(b,a) + \int_r^{a+b}\frac{a}{r}\Delta P\,dr\right] \tag{6.8}$$

(iii) For $r < a-b$ (outer region I):

$$P_N(r,a) - P^{II} = \frac{2}{a}\left[\sigma^{II}(b,a) + \sigma^{in}(b,a) + \int_r^{a-b}\frac{a}{r}\Delta P\,dr\right] \tag{6.9}$$

σ^{II} can be calculated from Eqn (2.7) and σ^{in} from Eqns (3.14) and (4.15)–(4.18). ΔP is given by Eqn (5.13).

In Fig. 3 numerical results for $P_N - P^{II}$ vs. $(r-a)$ are presented for liquid argon/gas interfaces of different radii a. It is seen that even for the smallest droplet ($a = 50$ Å) there is a homogeneous bulk liquid phase (P_N = constant) in the interior of the droplet (we do not consider completely inhomogeneous droplets of extremely small radii). The pressure difference $(P^I - P^{II})$ increases with decreasing drop size in accordance with the Laplace equation

$$P^I - P^{II} = \frac{2\sigma}{a} = \frac{2\gamma}{a} + \frac{B}{a^2} \tag{6.10}$$

where $P^I = P_N(r=0,a)$.

Further we consider the water/gas interface. For the Hamaker constant we

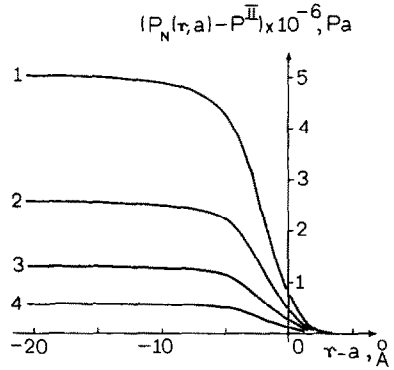

Fig. 3. Normal pressure distribution $P_N(r,a)$ across a liquid argon/gas spherical interface ($T=84.3$ K): curve 1, $a=50$ Å; curve 2, $a=100$ Å; curve 3, $a=200$ Å; curve 4, $a=500$ Å.

took a value determined in experiments on thinning of free water films [24]. The calculated value, $\delta_0=1.59$ Å, (Table 2) is close to the estimates of Tolman [35], $\delta_0=0.99$ Å, and of Wingrave et al. [36], $\delta_0=1.1$ Å.

In Table 2 numerical results for the benzene/gas interface are also shown with a Hamaker constant calculated with the aid of values for ϵ^* and R^* given on p. 36 of Ref. [37].

In a similar manner, liquid normal saturated hydrocarbons were investigated. The Hamaker constants (Table 2) were calculated according to Eqns (6.1) and (6.3). We used data for the Lennard–Jones interaction parameters ϵ^* and R^* taken from Ref. [37]. In Ref. [37] the molecules of the paraffins were subdivided into elementary fragments which were treated just like separate molecules interacting through a Lennard–Jones potential [Eqn (6.2)]. As an elementary fragment a $-CH_2-CH_2-$ group, equal to a methane molecule CH_4, was taken (see p. 338 of Ref. [37]). The interaction energy ϵ_r^* of an elementary fragment in a molecule of r fragments was determined (pp. 339, 340 and Table 16.18.1 on p. 341 in Ref. [37]). The calculations were carried out using the experimental Lennard–Jones parameters for liquid methane (Eqn (16.18.1) in Ref. [37]). Two sets of values of ϵ_r^* were obtained in Ref. [37] for saturated hydrocarbons from C_3H_8 to $C_{19}H_{40}$. The first set resulted from compressibilities and the second from molar enthalpies of liquid paraffins (Figs. 16.8.3 and 16.8.4 on p. 346 in Ref. [37]). We utilized the data from compressibilities since they had been determined under isothermal conditions. Besides, we interpolated for even numbers of C atoms between the values given in Ref. [37] for hydrocarbons with uneven number of C atoms. Correspondingly, the number density ρ_1 in Eqn (6.1) was set to be equal to the number of elementary fragments per unit volume. The results are presented in Table 2. The surface tension at a flat hydrocarbon/gas interface γ_0 is taken from experiments [38].

The Tolman length δ_0 is found to be almost constant for all the paraffins

studied, $\delta \approx 4.6$ Å. The interfacial bending moment at a flat hydrocarbon surface, B_0, ranges from 15 to 26 pN, being greater for liquids of larger Hamaker constant.

It should also be noted that the half-width of the transition region b has an approximately constant value: $b = 7.2$–7.3 Å for the liquid paraffins studied. Having in mind Eqn (4.19), we checked this result by plotting the experimental surface tension at a flat interface γ_0 vs. the calculated Hamaker constant A in Fig. 4. A straight line was obtained with a slope of $1.87 \cdot 10^{13}$ cm^{-2} (the data for γ_0 are measured at 20 °C).

A similar linear relationship between γ_0 and A has been recently reported as an empirically observed feature of systems with predominating Lifshitz–van der Waals (i.e. dispersion) interactions [28]. This is exactly the case of the liquid paraffins where only dispersion interactions exist. The empirical factor of proportionality was found to be $3.32 \cdot 10^{13}$ cm^{-2} [28] for a temperature of 25 °C.

Finally, we calculated the curvature dependence of the mechanical surface tension σ from Eqns (5.9) and (5.2), of the thermodynamic surface tension γ from Eqns (5.11), (5.2) and (5.8), of the bending moment B from Eqn (1.1) and of the distance $\delta = a - a_s$ with a_s being the radius of the surface of tension. The last was determined from the relation [15]

$$a_s = a\left(\frac{\gamma - B/a}{\sigma}\right)^{1/3}; \qquad \delta = a - a_s \tag{6.11}$$

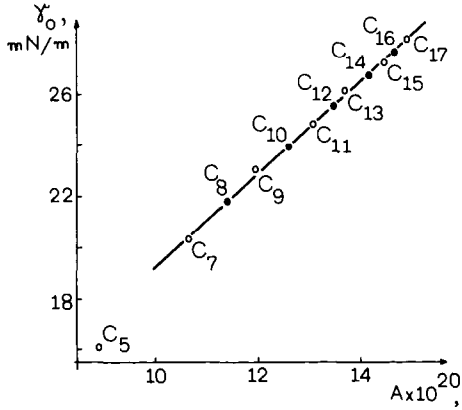

Fig. 4. Experimental surface tension γ_0 for liquid paraffins vs. the calculated Hamaker constant (Eqns (6.1) and (6.3)). Full circles correspond to hydrocarbons with an even number of C atoms for which the interaction parameter ϵ^* has been interpolated between the values for hydrocarbons with an odd number of C atoms, given in Ref. [37]. Open circles correspond to the latter values; $T = 20$ °C.

(For the sign of the curvature see Eqn (1.1) and thereafter.) Numerical data are presented in Figs. 5 and 6 for water/gas and *n*-decane/gas interfaces.

It is seen that for both interfaces the dependence of the mechanical surface tension σ on the curvature is linear. On the contrary, the thermodynamic surface tension γ exhibits deviations from the linear behavior, the latter corresponding to the Gibbs–Tolman equation [Eqn (1.3)]. These deviations are due to the non-linear term in Eqn (5.10) but its magnitude is fairly small (see Figs. 5(a) and 6(a)). The mechanical and the thermodynamical surface tensions σ and γ are observed to differ appreciably at radii below 1000 Å, owing to the presence of the bending moment B (see Eqn (1.1) and Figs. 5(a) and 6(a)). For the *n*-decane/gas interface this difference amounts up to 10% of the value of γ at $a=50$ Å.

Since σ and γ decrease as the curvature of the interface increases, positive values of B and δ are obtained. Both the bending moment B and the distance δ between the equimolecular surface and the surface of tension turn out to depend weakly on the radius a. The maximum deviations from the limiting values on a flat interface are less than 15% at $a=50$ Å.

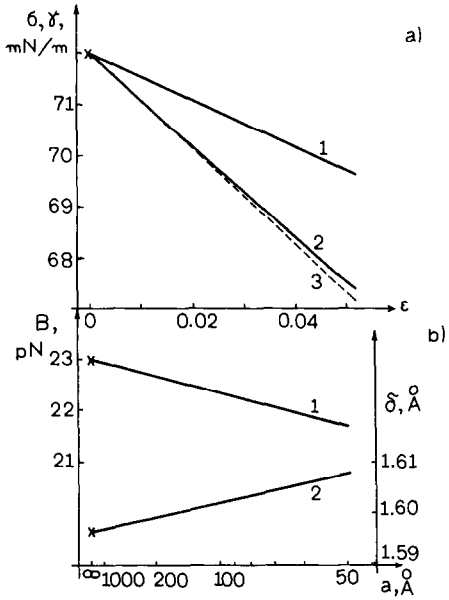

Fig. 5. Curvature dependence of the mechanical and thermodynamical surface tensions, bending moment and Tolman length for a water/gas interface. (a) Curve 1, the mechanical surface tension σ; curve 2, the thermodynamical surface tension γ; curve 3, a straight line corresponding to the Tolman equation [Eqn (1.5)]; $\epsilon=b/a$. (b) Curve 1, the interfacial bending moment B, curve 2, the Tolman length, $\delta=a-a_s$.

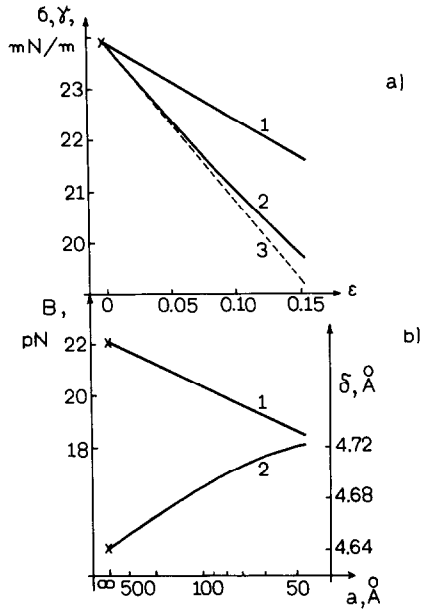

Fig. 6. Curvature dependence of the mechanical and thermodynamical surface tensions, bending moment and Tolman length for an *n*-decane/gas interface. The notation is the same as in Fig. 5.

6.2 Oil/water interfaces

We will next consider liquid/liquid interfaces between hydrocarbons (normal paraffins and benzene) and water. For the sake of definiteness we shall suppose the oil to be inside the droplet (phase I). The compound Hamaker constant A was calculated from Eqn (2.8) by using the data for the liquid/gas Hamaker constants presented in Table 2. We used the Hamaker assumption

$$\alpha_{12} = \sqrt{\alpha_{11}\,\alpha_{22}} \tag{6.12}$$

to determine α_{12}. The resulting values of A are given in Table 3. Experimental measurements on equilibrium planar films of different hydrocarbons in water, stabilized by various surfactants, gave a compound Hamaker constant A ranging from 0.3 to $1.5 \cdot 10^{-20}$ J [39], which is close to the values of A in Table 3.

The values of the second constant A_1, together with the results for b, δ_0 and B_0, calculated from Eqns (2.9), (4.19), (5.3) and (5.4) respectively, are also presented in Table 3, where γ_0 is the experimental interfacial tension (taken from Ref. [38]) at the plane interface hydrocarbon/water.

It is seen that δ_0 is negative and of the order of 5 Å. In view of our curvature sign convention for oil drops in water (see the comments after Eqn (1.1)) this means that the surface of tension is located in the oil phase. This is not surprising since oil is more "dense" than water with respect to the van der Waals

TABLE 3

Liquid-water interfaces (at 20°C)

Phase I	$A \cdot 10^{20}$ (J)	$A_1 \cdot 10^{20}$ (J)	γ_0 (mN m^{-1})	b (Å)	$-\delta_0$ (Å)	$-B_0 \cdot 10^{11}$ (N)
Benzene	8.599	14.82	35.0	4.94	7.75	5.425
n-C_5H_{12}	0.743	2.571	49.0	1.23	4.65	4.557
n-C_7H_{16}	1.308	3.734	51.2	1.59	4.82	4.936
n-C_8H_{18}	1.579	4.244	51.7	1.74	4.89	5.056
n-C_9H_{20}	1.791	4.631	52.0	1.85	4.94	5.138
n-$C_{10}H_{22}$	2.048	5.084	51.2	1.99	5.07	5.192
n-$C_{11}H_{24}$	2.236	5.408	52.5	2.06	5.05	5.303
n-$C_{12}H_{26}$	2.407	5.699	52.9	2.13	5.08	5.375
n-$C_{14}H_{30}$	2.708	6.199	53.3	2.25	5.14	5.479
n-$C_{16}H_{34}$	2.942	6.581	53.8	2.33	5.19	5.584

interactions (i.e. oil has a larger Hamaker constant than water). Therefore the surface of tension occurs in the more "dense" phase, just as it is in the case of liquid/gas interfaces. Similar observations have been reported for emulsion systems consisting of oil droplets in a mixture of water and methyl alcohol [40,41]. For instance, experimental measurements in a system of tribromomethane in water plus methyl alcohol [40] showed that Eqn (1.3) holds with $|\delta_0| = 2.4$ Å (with the surface of tension in the oil phase).

Unlike the case of liquid paraffin/gas interfaces, for paraffin/water interfaces the half-width b of the transition region depends on the paraffin chain length (see Table 3). A pot of b vs. the Hamaker constant A in a double-logarithmic scale is shown in Fig. 7. The parameter b increases as the Hamaker constant increases, with the dependence being a power function. From Eqn (4.19), used for the calculation of b, one obtains

$$\ln b = \text{constant} + \tfrac{1}{2} \ln A - \tfrac{1}{2} \ln \gamma_0 \qquad (6.13)$$

Then the plot in Fig. 7 implies that $\ln \gamma_0$ must be also a linear function of $\ln A$. The slope of the straight line in Fig. 7 together with Eqn (6.13) gives $\gamma_0(A) = \text{constant} \cdot A^{0.071}$. Most probably this non-linear dependence (cf. the linear dependence in Fig. 4) is due to the presence of polar interactions between the two phases.

Further, by means of Eqn (5.13) we calculated the anisotropy ΔP of the pressure tensor distribution in emulsion-type systems of oil in water. The results for n-decane/water and benzene/water interfaces are compared in Figs 8 and 9 with the corresponding curves for liquid/gas interfaces (i.e. oil/gas and gas/water) at the same radius, $a = 1000$ Å. For liquid/gas interfaces (curves 1 and 2) the pressure difference $\Delta P = P_N - P_T$ turns out to be positive throughout the system whereas for liquid/liquid systems ΔP takes negative values too. It

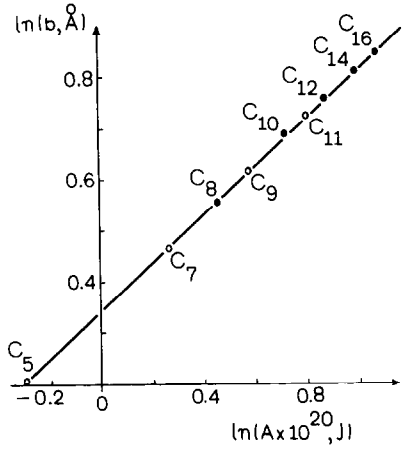

Fig. 7. Half-width of the transition region for liquid paraffin/water interfaces vs. the calculated compound Hamaker constant [Eqns (2.8) and (6.12)], in a double logarithmic scale. For the meaning of full and open circles see the caption to Fig. 4.

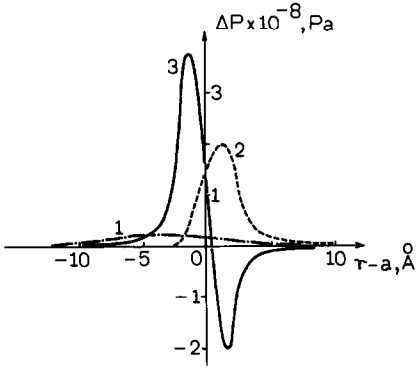

Fig. 8. Anisotropy of the pressure tensor distribution for a drop of radius $a = 1000$ Å: curve 1, a drop of n-decane in gas; curve 2, a gas bubble in water; curve 3, a drop of n-decane in water.

is worth noting that the region of negative ΔP is located at the side of the phase which is less "dense" with respect to the van der Waals interactions. In our case this is the water phase since it has a smaller Hamaker constant than the oil phase (Table 2).

From Eqns (5.9), (5.1), (1.1) and (6.11) we calculated the curvature dependence of σ, γ, B and δ of the interfaces n-decane/water (Fig. 10) and benzene/water (Fig. 11). The results are quite similar to those obtained for liquid/gas interfaces (see Figs. 5 and 6). Again B and δ exhibit a slight dependence on the radius a. In accordance with the curvature sign convention (see Eqn (2.19) in Ref. [16]) the values of B are negative. B tends to bend the interface

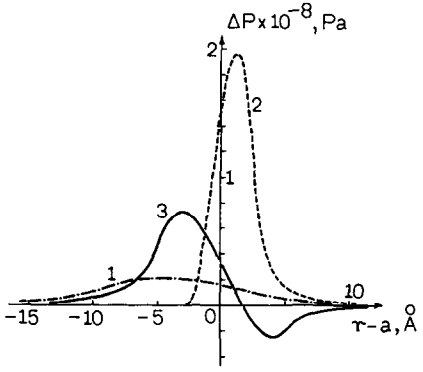

Fig. 9. Anisotropy of the pressure tensor distribution for a drop of radius $a = 1000$ Å: curve 1, a drop of benzene in gas; curve 2, a gas bubble in water, curve 3, a drop of benzene in water.

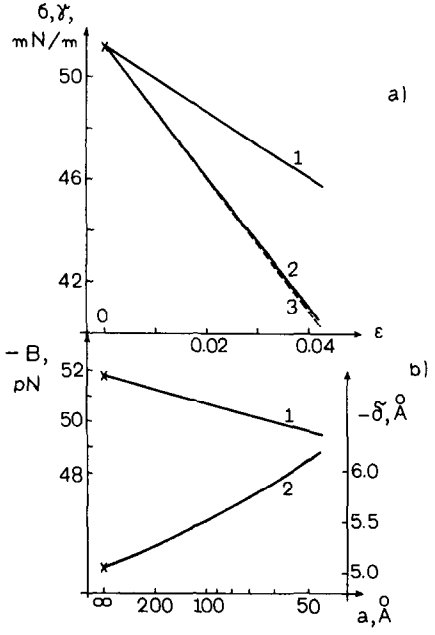

Fig. 10. Curvature dependence of the mechanical and thermodynamical interfacial tensions, bending moment and Tolman length for a *n*-decane/water interface. (a) Curve 1, the mechanical interfacial tension σ; curve 2, the thermodynamical interfacial tension γ; curve 3, a straight line corresponding to the Tolman equation [Eqn (1.5)]; $\epsilon = b/a$. (b) Curve 1, the interfacial bending moment B, curve 2, the Tolman length, $\delta = a - a_s$.

around the oil phase (i.e. around the phase of larger Hamaker constant) which resembles the results for liquid/gas interfaces where B, being positive, was tending to bend around the liquid phase (see Table 2).

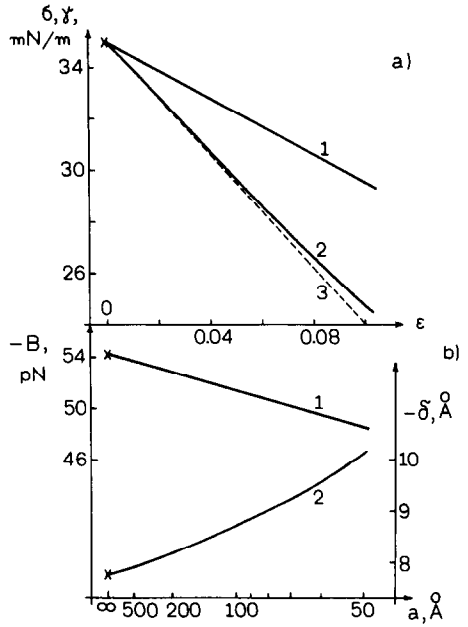

Fig. 11. Curvature dependence of the mechanical and thermodynamical interfacial tensions, bending moment and Tolman length for a benzene/water interface. The notation is the same as in Fig. 10.

A pronounced deviation between the mechanical and the thermodynamical interfacial tensions σ and γ is again observed at radii below 1000 Å (Figs 10(a) and 11(a)). Hence, for microemulsion systems it is important to discriminate between these two quantities.

7. CONCLUDING REMARKS

The model developed in this paper is aimed to express the mechanical properties of an interface in terms of the molecular interactions between the phases. The interfacial tension and the interfacial bending moment are related to the anisotropy $\Delta P = P_N - P_T$ of the pressure tensor distribution. Far apart from the interface, ΔP is calculated on the basis of the theory by Irving and Kirkwood [42] by using the long-range part of the Lennard–Jones interaction potential. In close vicinity to the interface a model expression for ΔP appeared to be necessary. Since we worked with the equimolecular dividing surface, some thermodynamic relations allowed us to determine the unknown parameters in this model expression and to obtain the profile ΔP across the whole interfacial zone. A comparison of our results for the pressure distribution ΔP with statistical mechanical calculations and computer simulations of other authors shows that our model seems to be close to the reality.

The model demands three parameters to be known independently. The first is the surface tension on a flat interface, γ_0, and the others are the two Hamaker constants of the two neighboring phases. (To determine the compound Hamaker constant we also used Eqn (6.12).) Having known these constants for some liquid/gas and oil/water interfaces, we calculated a full set of mechanical characteristics of the interface and their curvature dependences: the mechanical surface tension σ, the bending moment B, the radius of the surface of tension a_s, etc. It is worthwhile noting that simple algebraic expressions have been obtained for some interfacial properties. For example, the effective half-width of the interfacial transition zone, b, is connected with the Hamaker constant A and the surface tension γ_0 via Eqn (4.19); similar expressions are derived for the Tolman length δ_0 [Eqn (5.3)] and for the interfacial bending moment B_0 [Eqn (5.4)]. Also explicit expressions for calculating the variation of the pressure tensor components across the interfacial zone are derived (see Eqn (5.13)).

The numerical results show that the bending moment plays an important role in the mechanics of interfaces. In particular, it can lead to a pronounced deviation between the mechanical and the thermodynamical interfacial tensions (see Figs. 5(a), 6(a), 10(a) and 11(a)). Therefore, for highly curved interfaces one should distinguish between these two interfacial characteristics.

In spite of the fact that our model is developed for interfaces without adsorbed surfactant molecules, our results can also be applied to more complicated microemulsion systems, which contain adsorbed surfactant and cosurfactant molecules as well as electrolyte in the aqueous phase. Indeed, as demonstrated in Ref. [16], the total interfacial bending moment can be represented as a sum of several components. One of them (it is denoted B_p in Ref. [16]) accounts for the van der Waals interactions between the two phases in the case when all surfactant and cosurfactant molecules are removed from the interface. In fact this component of the bending moment is calculated in the present paper. Its magnitude (see Tables 2 and 3) is of the order of 10 pN, so it can be comparable to the electrostatic and steric components of the interfacial bending moment (see Ref. [16]). Thus, similarly to the disjoining pressure in thin films (see for example Ref. [43]) the interfacial bending moment of a microemulsion drop turns out to be a superposition of van der Waals, electrostatic and steric components.

ACKNOWLEDGEMENTS

This work was supported by the Bulgarian Committee for Science and Higher Education.

REFERENCES

1 K. Motomura, Adv. Colloid Interface Sci., 12 (1980) 1.
2 J.Th.G. Overbeek, G.J. Verhoeckx, P.L. de Bruyn and H.N.W. Lekkerkerker, J. Colloid Interface Sci., 119 (1987) 422.
3 E. Ruckenstein, in K.L. Mittal and B. Lindman (Eds.), Surfactants in Solution, Vol. 3, Plenum, New York, 1984, p. 1551.
4 E. Ruckenstein, J. Colloid Interface Sci., 114 (1986) 173.
5 P.G. de Gennes and C. Taupin, J. Phys. Chem., 86 (1982) 2294.
6 C.A. Miller, J. Dispersion Sci. Tech., 6 (1985) 159.
7 S. Mukherjee, C.A. Miller and T. Fort, Jr., J. Colloid Interface Sci., 91 (1983) 223.
8 N.D. Denkov, P.A. Kralchevsky, I.B. Ivanov and C.S. Vassilieff, J. Colloid Interface Sci., in press.
9 J.G. Kirkwood and F.P. Buff, J. Chem. Phys., 17 (1949) 338.
10 T.L. Hill, J. Chem. Phys., 20 (1952) 141.
11 I.W. Plesner and O. Platz, J. Chem. Phys., 48 (1968) 5361.
12 S. Toxvaerd, Mol. Phys., 26 (1973) 91.
13 C.A. Croxton and R.P. Ferrier, J. Phys. C: Solid State Phys., 4 (1971) 2433.
14 P.A. Kralchevsky and T.D. Gurkov, Colloids Surfaces, 56 (1991) 101.
15 T.D. Gurkov and P.A. Kralchevsky, Colloids Surfaces, 47 (1990) 45.
16 P.A. Kralchevsky, T.D. Gurkov and I.B. Ivanov, Colloids Surfaces, 56 (1991) 149.
17 J.W. Gibbs, The Scientific Papers of J. Willard Gibbs, Vol. 1, Longmans Green, New York, 1906, reprinted by Dover, New York, 1961.
18 R.C. Tolman, J. Chem. Phys., 17 (1949) 333.
19 S. Ono and S. Kondo, in S. Flugge (Ed.), Molecular Theory of Surface Tension in Liquids, Handbuch der Physik, Vol. 10, Springer, Berlin, 1960.
20 J.S. Rowlinson and B. Widom, Molecular Theory of Capillarity, Clarendon Press, Oxford, 1982.
21 F.P. Buff, J. Chem. Phys., 23 (1955) 419.
22 A.H. Nayfeh, Perturbation Methods, Wiley, New York, 1973.
23 H.C. Hamaker, Physica, 4 (1937) 1058.
24 S. Nir and C.S. Vassilieff, in I.B. Ivanov (Ed.), Thin Liquid Films, Marcel Dekker, New York, 1988, p. 207.
25 A.H. Falls, L.E. Scriven and H.T. Davis, J. Chem. Phys., 75 (1981) 3986.
26 S.M. Thompson, K.E. Gubbins, J.P.R.B. Walton, R.A.R. Chantry and J.S. Rowlinson, J. Chem. Phys., 81 (1984) 530.
27 I.B. Ivanov and P.A. Kralchevsky, in I.B. Ivanov (Ed.), Thin Liquid Films, Marcel Dekker, New York, 1988, p. 49.
28 C.J. van Oss, M.K. Chaudhury and R.J. Good, Chem. Rev., 88 (1988) 927.
29 A.I. Rusanov and E.N. Brodskaya, J. Colloid Interface Sci., 62 (1977) 542.
30 M. Rao and B.J. Berne, Mol. Phys., 37 (1979) 455.
31 S.J. Hemingway, J.R. Henderson and J.S. Rowlinson, Faraday Symp. Chem. Soc., 19 (1981) 33.
32 S.J. Hemingway, J.S. Rowlinson and J.P.R.B. Walton, J. Chem. Soc., Faraday Trans. 2, 79 (1983) 1689.
33 J.O. Hirschfelder, C.F. Curtiss and R.B. Bird, Molecular Theory of Gases and Liquids, Wiley, New York, 1954.
34 F.P. Buff, in S. Flugge (Ed.), The Theory of Capillarity, Handbuch der Physik, Vol. 10, Springer, Berlin, 1960, p. 281.
35 R.C. Tolman, J. Chem. Phys., 17 (1949) 118.

36 J.A. Wingrave, R.S. Schechter and W.H. Wade, in A.I. Rusanov and F.C. Goodrich (Eds.), The Modern Theory of Capillarity, Khimia, Leningrad, 1980, p. 244 (in Russian).
37 I. Prigogine, The Molecular Theory of Solutions, North Holland Publishing Company, Amsterdam, 1957.
38 A.A. Abramson and E.D. Shchukin (Eds.), Surface Phenomena and Surface-Active Substances, Khimia, Leningrad, 1984 (in Russian).
39 J. Requena and D.A. Haydon, Proc. R. Soc. London, Ser. A, 347 (1975) 161.
40 A.E. Nielsen and S. Sarig, J. Crystal Growth, 8 (1971) 1.
41 A.E. Nielsen and P.S. Bindra, Croat. Chem. Acta, 45 (1973) 31.
42 J.H. Irving and J.G. Kirkwood, J. Chem. Phys., 18 (1950) 817.
43 B.V. Derjaguin, Theory of Stability of Colloids and Thin Films, Nauka, Moscow, 1986 (in Russian); Plenum, New York, 1989.